Biomedicine & Pharmacotherapy 128 (2020) 110294

Contents lists available at ScienceDirect

Biomedicine & Pharmacotherapy

journal homepage: www.elsevier.com/locate/biopha

Original article

Antitumor effect of cell therapy with mesenchymal stem cells on murine melanoma B16-F10

Fernanda Carrilho de Menezes[a], Laertty Garcia de Sousa Cabral[b], Maria Carla Petrellis[b], Cyro Festa Neto[a], Durvanei Augusto Maria[b,*]

[a] Department of Dermatology, Clinics Hospital-FMUSP, Sao Paulo University, Av. Dr Eneias de Carvalho, 255, Sao Paulo, 05403-000, Brazil
[b] Molecular Biology Laboratory, Butantan Institute, Av. Dr. Vital Brasil, 1500, Butantan, Sao Paulo, 05599-000, Brazil

ARTICLE INFO

Keywords:
Tumor
Melanoma
Mesenchymal stem cells
Immunomodulatory
Apoptosis

ABSTRACT

In this study, the antitumor and immunomodulatory effects of mesenchymal stem cells (MSC) obtained from bone marrow in the treatment of dorsal melanoma B16-F10. The MSC cells were obtained from the bone marrow of isogenic C57BL/6J mice, characterized and inoculated by two routes, intratumor (it) and intravenous (iv). The hematological profile, expression markers and receptors, phases of the cell cycle and mitochondrial electrical potential were evaluated by flow cytometry. The dorsal tumor mass showed a significant reduction after treatment by the two routes of administration with a significant effect by the intravenous route. MSC showed immunomodulatory potential and did not induce an increase in the markers involved in tumor control and progression. The number of cells in the sub-G1 phase increased significantly after treatments compared to the control group. The percentage of cells in phases G0/G1, S and G2/M decreased, with only the group (it) showing a significant reduction. The intratumor group showed a significant decrease in the G2/M phase. Treatment with MSC provided a significant decrease in the percentage of metabolically active tumor cells, demonstrating its intrinsic effect in the control of cell proliferation. Regarding the mechanism of cell death, MSCs modulated the expression of proteins involved in the regulation of the cell cycle, angiogenesis receptors and pro-apoptotic proteins by intrinsic and extrinsic routes. Therefore, the use of undifferentiated MSC, administered intratumor and intravenous is possibly a promising treatment for melanoma.

1. Introduction

Cutaneous melanoma (CM) is a malignant transformation of melanocytes, melanin producing cells normally located in the epidermis, dermis or mucosal epithelium; or melanocytic nevus cells, such as atypical or congenital nevi; or rarely, of melanocytes in visceral sites [1,2], being one of the most aggressive skin tumors. The incidence of CM has been increasing in the last two decades, especially in light-skinned individuals [3,4].

Melanoma accounts for about 1% of all skin cancer cases, accouting for the vast majority of skin cancer deaths [5]. The number of new cases are estimated at about 420.000 worldwide. The estimate number for sub-registration may be of 640 thousand new cases, for Brazil 2018–2019 biennium, of 170.000 new cases [6].

Despite the efforts made, the best CM therapy is still early diagnosis, the use of chemotherapeutic agents alone or in combination is reserved for metastatic disease, and the adjuvant therapies employed have not been able to decisively influence survival, generating short response duration and effectiveness of less than 5% of the cases used.

Immunotherapy is the latest advancement in cancer therapy. Thanks to the remarkable clinical results of checkpoint inhibitors and the approval of the US Food and Drug Administration (FDA) in 2017, CAR-T cells are a promising new therapy that offers significant advantages compared to conventional immunotherapies for the treatment of tumor [7,8].

Mesenchymal stem cells (MSCs) have become the focus of therapeutic attention because of their immunomodulatory potential. By direct contact of the MSC with specialized cells of a tissue or by the paracrine interaction with the interferon-gama (INF-γ), producing immune cells, triggering the release of several factors such as prostaglandins (PGE2), factor (TGF-β), hepatocyte growth factor (HGF), and the indoleamine 2,3-dioxygenase (IDO), enzyme that will act on lymphocytes and Antigen Presenting Cells (APC). One of the functions of MSC in organs and tissues is to replace damaged cells, thus, these cells function as tissue repairers, responsible for maintaining the integrity and homeostasis of organs [9,10].

* Correspondence author at: Av. Dr. Vital Brasil, 1500, Butantan, Sao Paulo, 05599-000, Brazil.
E-mail address: durvanei@usp.br (D.A. Maria).

https://doi.org/10.1016/j.biopha.2020.110294
Received 1 November 2019; Received in revised form 14 May 2020; Accepted 16 May 2020

MSCs have antitumor, immunoregulatory potential and show pathotropic migratory characteristics, accrediting them as potential tools for application in tumor therapy targeted

delivery vectors [11–13]; MSC is considered an excellent candidate for application in tumor cell therapy because it is obtained from the patient; easy to isolate and manipulate in laboratory [14–18]. MSC have unique properties, such as migration toward cancer cells, secretion of bioactive factor, and immunosuppression which tumor targeting and circumvent obstacles currently impede gene therapy strategies. Preclinical stem cell-based strategies show great promise in targeted anticancer therapy applications. The scarcity of studies in the use of cell therapy in the treatment of melanoma motivated the development of this experimental work, so that the knowledge of the mentioned factors can help in the development of safe clinical protocols that could be used in humans. We sought to evaluate the antitumor and immunomodulatory effects of undifferentiated mesenchymal bone marrow stem cells in the treatment of murine melanoma B16-F10 model in mice.

2. Materials and methods

2.1. Reagents

The reagents involved in this study were purchased from Sigma Aldrich Chemical Co. (St.

Louis, MO, USA).

2.2. Cell culture

The melanoma murine cells (B16-F10) (ATCC® CRL-6475™) used in this study belong to the cell bank of the Molecular Biology Laboratory of the Butantan Institute, under the responsibility of Prof. Dr. Durvanei Augusto Maria. Cells were cultured in RPMI-1640, pH = 7.2 supplemented with 10% inactivated fetal bovine serum (FBS), 2 mM L-glutamine and 1% antibiotics (10.000 IU/ml penicillin and 10 mg/ml streptomycin). Tumor cells were incubated in 75 cm2 culture flasks under moist atmosphere conditions of 5% CO2 at 37 °C until reaching approximately 90% confluency. Prior to the execution of the experiments, the cells were counted in the haemocytometry Neubauer chamber using Tripan blue dye (1%), which does not penetrate into viable cells which have intact cell membrane. Only cells with viability equal to or greater than 90% were used in the assays.

2.3. Animals

All animal experiments were in accordance to The Animal Experimentation Ethics Committee (CEEA) of the Butantan Institute, Protocol Number 928/12. Thirty 6 to 8 week-old C57BL/6 J adult and clinically healthy female mice, weighing approximately 25 g were obtained from the Central Bioterium and housed at the Bioterium of the Scientific Development Division of the Butantan Institute. The murine melanoma cell line (B16-F10) originated from *Mus musculus* C57.

2.4. Isolation and culture of mesenchymal stem cells from C57BL / 6 J mice

After anesthesia with a solution containing ketamine hydrochloride 35 mg/kg and xylazine hydrochloride 80 mg/kg, according to protocol described in the Use of Experimental Animals at Johns Hopkins - Guide to the Care and Use of Experimental Animals - cervical displacement was performed. Trichotomy followed by asepsis with detergent iodine, alcohol and polyvinylpyrrolidone were performed on the left femoral region. Afterwards, the animals were positioned in left lateral decubitus position, the femoral joint was flexed and then, a Rosenthal 6 needle, 16 G x15 cm, was inserted in the femoral head region by means of rotational movements. After penetrating into the cortical bone, 2 ml of the bone marrow were aspirated into a 10 ml syringe containing 0.1 ml of sterile saline with sodium heparin

(5000 u/ml). During the procedure, slow movements were made with the syringe to homogenize the blood, preventing the formation of clots. For isolation and better separation of the mesenchymal stem cells, the samples were diluted in 2 ml of phosphate buffer solution (PBS) and centrifuged at 900 rpm for 10 min. After centrifugation, the supernatant was discarded and the pellet resuspended in 1 ml of RPMI medium, pH = 7.0, supplemented with 20% inactivated fetal bovine serum (FBS), 2 mM L-glutamine and 1% antibiotics (10.000 IU/mL penicillin and 10 mg/ml streptomycin). Cells were evaluated in number and viability by Tripan blue staining, in the Neubauer hematocytometric chamber by using a light field microscope. The cell concentration was adjusted to 10^5, 10^4 and 10^3 and maintained in 25 cm^2 flasks in an incubator containing 5% CO_2 humid atmosphere at 37 °C. The selection and expansion of the mesenchymal stem cells were performed by successive repackage up to the 10th culture pass. MSCs grow in monolayer, adhered to the surface of the culture dish. Cell subculture was performed from confluent cultures, around 3 days, and expanded after trypsinization of the cells. Subsequently, markers CD34, CD105, CD90, CD8, CD44, CD43, IL- 6R, Cyclin D1, TRAIL-DR4, Caspase-8, Bax, Bad and Caspase-3 were quantified by flow cytometry.

2.5. Experimental protocol

The animals were submitted to manual restraint and trichotomy in the dorsal region for posterior inoculation of B16-F10 murine melanoma cells. Cells were inoculated at 5 × 104 subcutaneously using a 1 ml syringe and hypodermic needle (13 × 0.30 mm). After the 20th day of inoculation of the tumor cells, the animals were randomized into 3 different treated groups, respectively (n = 10 animals per group). Control group did not receive treatment. Tumor + MSC (iv) treated group, the animals were treated with MSC at a concentration of 10^6 via intravenous for 28 days. Tumor + MSC (it) treated group was treated with MSC at a concentration of 10^6 via intratumor for 28 days. The weight and hematological profile were evaluated weekly. After the treatment period, the animals were sacrificed, the tumor mass and internal organs (lung, spleen, kidneys, lymph nodes and liver) and blood were collected.

2.6. Analyzes of tumor weight and volume of melanoma-bearing mice

During the experimental period, the weight and dimensions of the dorsal tumor mass were performed weekly. Tumor mass measurement was performed using a digital caliper (Mitutoyo, measuring 0.01 mm) and photo documented on a digital camera. Subsequently, analyzes were performed using the formula for measuring the tumor volume, as described below.

Tumor volume (mm3) = length (mm) x [Width (mm)] 2/2

2.7. Analysis of hematological profile

The hematological profile of the melanoma-bearing animals of the treatment groups was determined on the 1th, 7th, 14th and 28th day after inoculation of the tumor cells. Peripheral blood samples were collected from the submandibular plexus and direct counts of total leukocytes (1/20 dilution in Turk's solution), platelets (1/20 dilution in ammonium oxalate) and erythrocytes (1/1000 dilution in PBS), in a haemocytometry Neubauer chamber. The differential percentage of leukocytes was counted on a blood smear stained by the panoptic method (methanol, eosin, hematoxylin), with 100% being the total leukocytes obtained by the direct method. For reticulocyte count, 20 µl of blood was mixed with 20 µl of bright cresyl blue dye, and incubated at 37 °C for 20 min, and then, the smears were run, and the optical microscope readout in an immersion. Values were expressed as mean

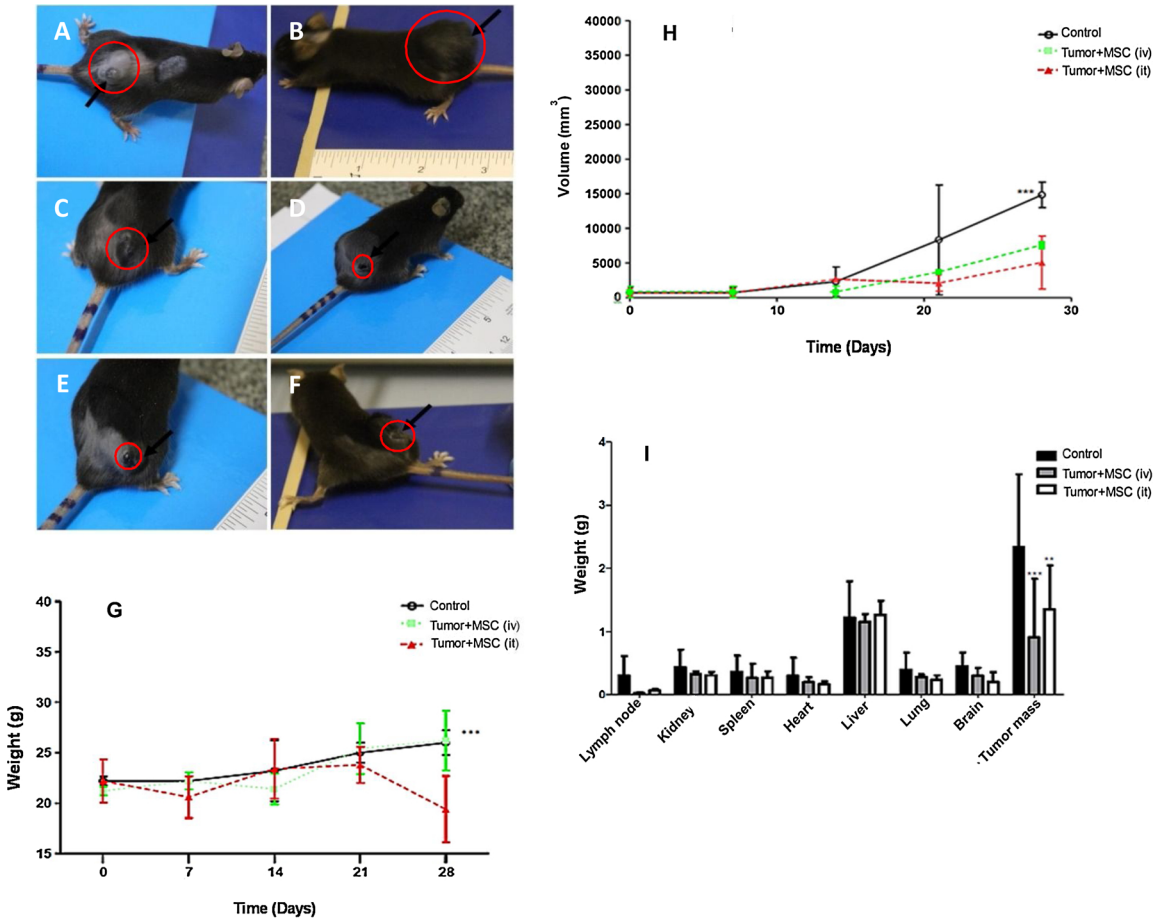

Fig. 1. Tumor volume of the animals and determination of the weight of the organs. Melanoma-bearing C57BL / 6 J mice were treated with MSC by the intratumoral and intravenous via once a week for 28 days. (A and B) Tumor control group; (C and D) Group treated with intravenous MSC; (E and F) Intratumoral MSC-treated group (G) Data of the weight of the animals of Tumor + MSC (it) and Tumor + MSC (iv) treated groups and Control group. (H) Data of the tumor volume of the animals of Tumor + MSC (it) and Tumor + MSC (iv) treated groups and Control group. (I) Determination of the weight of the organs of animals of t of Tumor + MSC (it) and Tumor + MSC (iv) treated groups and Control group. Tumor mass (arrow).

percentages by field.

2.8. Analysis of the expression of the markers "in vivo" by Flow Cytometry

The tumor mass of mice bearing murine melanoma B16-F10 was collected after euthanasia on day 28, macerated, the tumor cells were obtained by collagenases type III digestion and fixed in FACSFlow buffer with paraformaldehyde (2.5%) for 1 h. The cells were permeabilized with Triton X-100 (0.1%) for 30 min at 4 °C, only for analyzes of the cyclin D1, Bad, Bax, IL-6R, TRIAL-DR4, VEGF-R1, VEGF-R2, caspase 3 and 8 markers. Cell suspensions were washed and suspended in FACSflow buffer. Then, 1 µg of the specific primary antibody was added to the markers described below. After 1 h of incubation, the cells were centrifuged at 1500 rpm for 10 min, followed by incubation with anti-mouse IgG antibody (Alexa-Fluor® 488 - Invitrogen) for 1 h at 4 °C, protected from light. After specific binding of the antibodies, the cells were washed and suspended in 200 µl of FACSFlow buffer. Cell fluorescence was analyzed on a FACS Calibur flow cytometer (Becton Dickinson, San Jose, CA, USA) using Cell Quest and WinMDI ver 2.9 software, which were employed for acquisition and histogram analysis. Cell auto-fluorescence was measured using flow cytometry, using cells incubated without fluorochrome-labeled antibodies. The fluorescence intensity was measured for the fluorochrome with light at the maximal wavelength. The expression of different surface antigens was determined using the antibodies described above, and labeling was performed according to the supplier's recommendations.

2.9. Analysis of the cell cycle phases "in vivo" by Flow Cytometry

The tumor mass of mice bearing B16-F10 murine melanoma was collected after euthanasia on day 28, macerated and fixed in 1 ml of cold alcohol 70%, and stored at −20 °C. At the time of analysis, the cells were centrifuged at 1800 rpm for 5 min and washed in PBS. The cells were then centrifuged again and resuspended in 100 µl of FACS buffer containing 1.8 µl propidium iodide (PI) solution, 0.1% Triton X-100 and 4 mg/ml RNAse-A diluted in PBS and incubated for 1 h at 4 °C, protected from light. After this time, 1 ml of FACS buffer was added, followed by centrifugation at 1800 rpm, for 5 min. Subsequently, the supernatant was discarded and the pellet was suspended in 300 µL of FACS buffer. Samples were read on the FACScalibur (Fluorescence Activated Cell Analyzer - Becton and DicKinson, USA) flow cytometer, in FL2-H fluorescence channel, adjusted for 10.000 events. The results were analyzed using ModFit LT 3.2 (Becton Dickinson) software. The histograms show the cells distributed in the different phases of the cell cycle: Sub-G1; G0/G1, S and G2/M, which were expressed as mean ± standard deviation (SD).

2.10. Histopathologic analyses

The samples were sent to the Paulista Laboratory of Clinical Dermatopathology, Jardim Paulista, SP, Brazil, for routine histological processing (Hystotec). 5 µm histological sections of all the organs removed were stained with hematoxylin and eosin (HE) and examined

under light microscopy. In the parenchyma of the various organs the following parameters were evaluated: presence, intensity and characteristics of the inflammatory response, predominant cell type in the exudate, fibroblast and vascular proliferation. As to intensity, the inflammatory response was subjectively classified as mild, moderate and marked. The samples of tumors were evaluated in: 1) size; 2) symmetry; 3) lateral delimitation; 4) maturation; 5) pagetoid dissemination; 6) necrosis / ulceration; 7) inflammatory infiltrate; 8) regression; 9) cellular atypia; 10) mitoses; 11) melanization; 12) proliferation of isolated cells. The histological sections were analyzed by a pathologist blind to all groups.

2.11. Statistical analyzes

Statistical analysis was performed with Graph Pad Prism software Version 5.0. The data were expressed as means ± SD and subjected to one-way ANOVA followed by Turkey-Kramer multiple comparison tests. p values < 0.05 were considered statistically significant.

3. Results

MSC administration in the cutaneous melanoma model modulated tumor growth. Fig. 1 represents weight and volume assessment data measured weekly over a period of 28 days. It was possible to observe through macroscopic analysis that there was a significant reduction in tumor volume after the treatment protocol period in the treated groups by both routes of administration (Fig. 1A–F). We observed that in the Control group and Tumor + MSC (it) treated group, weight gain was observed during the treatment period that is attributed to the development and growth of solid tumor mass. However, in the Tumor + MSC (iv) treated group, there was a weight reduction that was statistically significant when compared to the other experimental groups (Fig. 1G). Moreover, the macroscopic analysis showed a statistically significant reduction in tumor volume in the Tumor + MSC (it) (5.07 ± 3.82 mm^3) and Tumor + MSC (iv) (7.59 ± 5.05 mm^3) treated groups when compared to the control group at the end of treatment (Fig. 1H). After the treatment period, all internal organs and solid tumor mass were collected and weighed for the assessment of increase or decrease in size and weight. After the treatment period, all internal organs and solid tumor mass were collected and weighed for the assessment of increase or decrease in size and weight. There was statistically significant reduction in lymph node weight in the Tumor + MSC (it) and Tumor + MSC (iv) treated groups when compared to the control group. However, this reduction was not statistically significant, despite numerical differences. However, there was a statistically significant reduction in solid tumor mass volume in the Tumor + MSC (it) and Tumor + MSC (iv) treated groups, but this effect was more pronounced in the Tumor + MSC (iv) treated group (Fig. 1I).

The hematological profile evaluation data are shown in Fig. 2. Regarding the total number of erythrocytes, we can observe a statistically significant reduction in the total number of erythrocytes in the Tumor + MSC (it) and Tumor + MSC (iv) treated groups 4.7 ± 0.2 × 10^9/ml, when compared to reference values after the end of the treatment period. The mean value for the control group over the same 28-day period was 4.5 ± 0.9 × 10^9/ml (Fig. 2A). Regarding the data on the total number of leukocytes, no statistically significant changes were found in the control group during the treatment period, obtaining average values of 31.1 ± 1.5 × 10^9/ml on the 28 day. However, there is a statistically significant increase when compared to the reference values. We found a statistically significant reduction in the total number of leukocytes in Tumor + MSC (it) (23.6 ± 1 × 10^9/ml-7th day of treatment)/(20 ± 1.4 × 10^9/ml-28th day of treatment) and Tumor + MSC (iv) treated groups (16.9 ± 2.1 × 10^9/ml-7th day of treatment)/(17.0 ± 1.2 × 10^9/ml-28th day of treatment) when compared to the control group (Fig. 2B). Data from mean platelet count values, a statistically significant increase was found in the Tumor + MSC (it) and Tumor + MSC (iv) treated groups (108,567 ± 1 × 10^5/ml-21st day of treatment) when compared to baseline values. However, there was a statistically significant reduction in the Tumor + MSC (it) and Tumor + MSC (iv) treated groups (94.400 ± 1,102 × 10^5/ml-28th day of treatment) when compared to the control group (148.000 ± 1.240 × 10^5/ml-28th day of treatment) (Fig. 2C). Data on reticulocyte counts showed a statistically significant increase in the percentage of reticulocyte counts in Tumor + MSC (it) (2.5 ± 0.1%–28th day of treatment) and Tumor + MSC (iv) (2.8 ± 0.2%-28th day of treatment) treated compared to the control group (2.1 ± 0.1%–28th day of treatment). These findings reflect the degree of anemia found in the number of erythrocytes in response to the modulating effect induced by MSCs (Fig. 3C). In assessing the presence of eosinophils, we found no statistically significant difference between the other experimental groups during the 28-day treatment period (Fig. 2D). Regarding the data found for neutrophils, there was a significant increase in the Tumor + MSC (it) and Tumor + MSC (iv) treated groups when compared to the reference values after the end of the treatment period (Fig. 2E). Based on the number of basophils, it was observed that there was a significant increase in the percentage Tumor + MSC (it) (2.6 ± 0.1%–28 day of treatment) and Tumor + MSC (iv) (2.3 ± 0.1%–28 day of treatment) treated. compared to the control group (1.6 ± 0.1%–28 day of treatment) (Fig. 2F). Lymphocyte assessment data for the Tumor + MSC (it) and Tumor + MSC (iv) treatments showed a significant reduction in lymphocyte counts for the 7, 21, and 28 day period (Fig. 2G). A significant reduction could be observed for both monocyte treatments. The treatment with the greatest reduction was Tumor + MSC (iv) (2.1 ± 0.1%–28 day of treatment) compared to the control (4.0 ± 0.1%–28 day of treatment) (Fig. 2H). There was no statistical significance for altering the percentage of eosinophils in any of the treatments (Fig. 2I).

The comparative assessment of marker expression levels is shown in Figs. 3 and 4. At CD34, CD105 and CD90 expression levels, we found a statistically significant decrease in Tumor + MSC (it) (32.5 ± 6.3% -CD34), (32.5 ± 6.3% -CD105), (71.0 ± 15.0% -CD90) and Tumor + MSC (iv) (18.0 ± 4.2%-CD34), (13.4 ± 5.2% -CD105), (38.5 ± 7.0% -CD90) when compared to the Control group (Fig. 3A, B, C). At CD8 expression levels, we found a statistically significant increase in the Tumor + MSC (it) treated group (32.8 ± 1.2%) when compared to the Tumor + MSC (iv) treated group and the Control group (Fig. 3D). CD44 and CD43 expression levels, a statistically significant decrease, were found in the Tumor + MSC (it) treated group (18.5 ± 7.0% -CD44), (15.0 ± 1.2% -CD43).) when compared to Tumor + MSC

(iv) treated group and control group (Fig. 3E and F). IL-6R, TRAIL-DR4 and BAD expression levels, a statistically significant increase in the Tumor + MSC (iv) treated group (42.4 ± 1.06% -IL-6r), (43.4 ± 2, 8% -TRAIL-DR4), (39.7 ± 7.0%) when compared to the Tumor + MSC (it) treated group and the control group (Fig. 3G–I). At levels of cyclin D1 expression, a statistically significant decrease was observed in the Tumor + MSC (it) (28.5 ± 2.1%) and Tumor + MSC (iv) treated groups (18.0 ± 5.6%).) when compared to the Control group; therefore, regulating cell cycle progression (Fig. 3H). Caspase-8, BAX and Caspase-3 expression levels, we found a statistically significant increase in Tumor + MSC (it) (30.0 ± 7.5% - Caspase-8), (41.5 ± 7.0% - BAX), (35.6 ± 7.0% - Caspase-3) and Tumor + MSC (iv) (28.0 ± 1.0% - Caspase-8), (34.0 ± 1.5% - BAX), (28.7 ± 3.0% - Caspase-3) treated groups when compared to the Control group (Fig. 3J–M). VEGF-R1 and VEGF-R2 expression levels were considerably reduced when compared to the control group. Tumor + MSC (iv) treatment showed a reduction for both VEGF-R1 (31.9 ± 1.8%) and VEGF-R2 (28.7 ± 8.3%) receptors for Tumor + MSC (it) the same was seen for VEGF-R1 (35.1 ± 3.8%) and VEGF-R2 (29.45 ± 9.62%) (Fig. 3N–O).

The treatments with MSCs were evaluated for the ability to modify

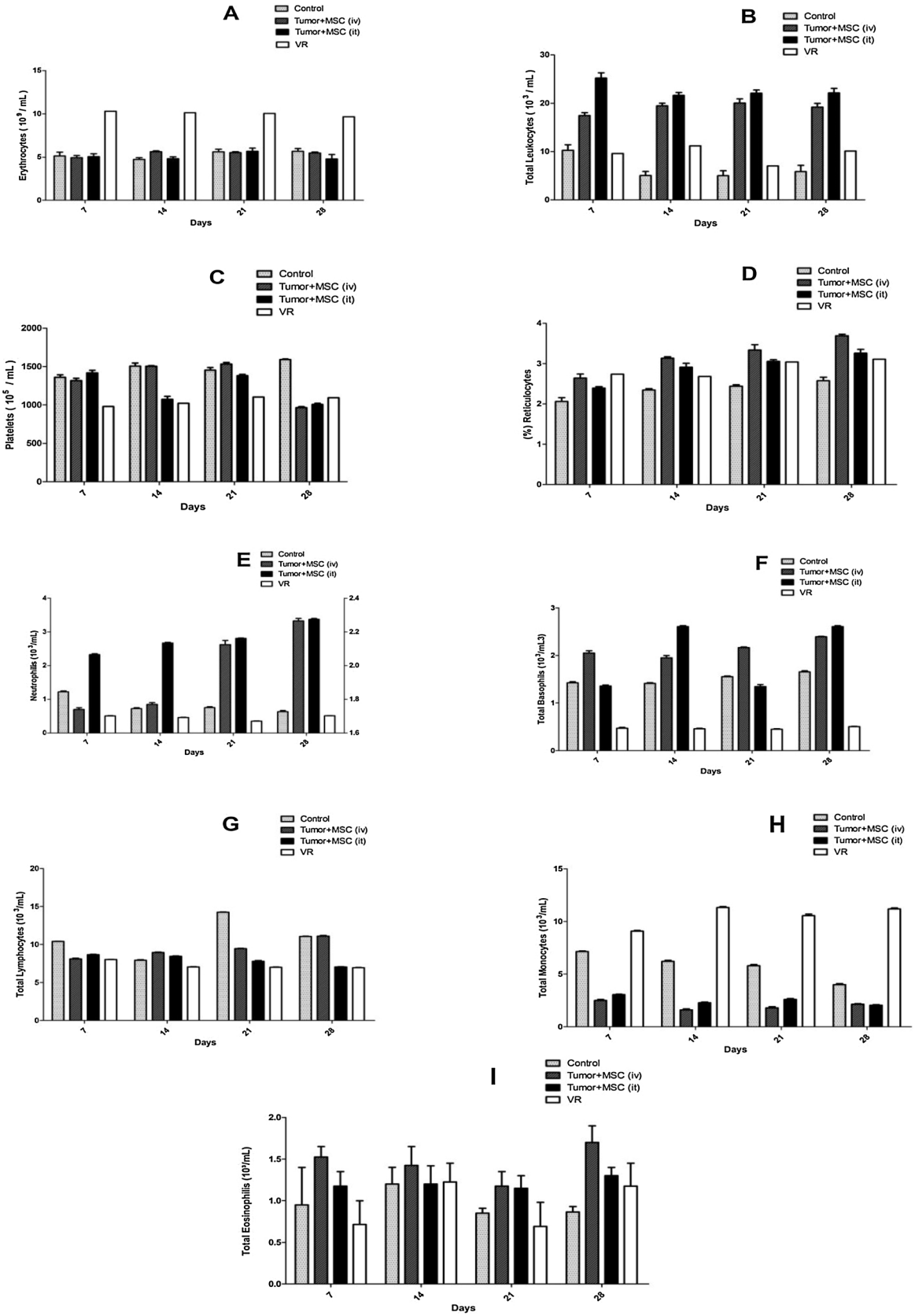

Fig. 2. Hematological profile data. (A) Red blood cell count parameter. (B) Total leukocyte count parameter. (C) Platelet count parameter. (D) Reticulocyte count parameter (E) Neutrophil count parameter (F) Basophil Total count parameter (G) Total Lymphocyte count parameter (H) Macrophage Total count parameter (I) Eosinophils Total count parameter. C57BL / 6 J mice bearing group melanoma were treated with intratumoral and intravenous MSC once weekly for 28 days and weekly hematological analyzes. Values are expressed as mean ± standard deviation SD from three independent experiments. Statistical significance level $p < 0.05$, ** $p < 0.01$ and *** $p < 0.001$.

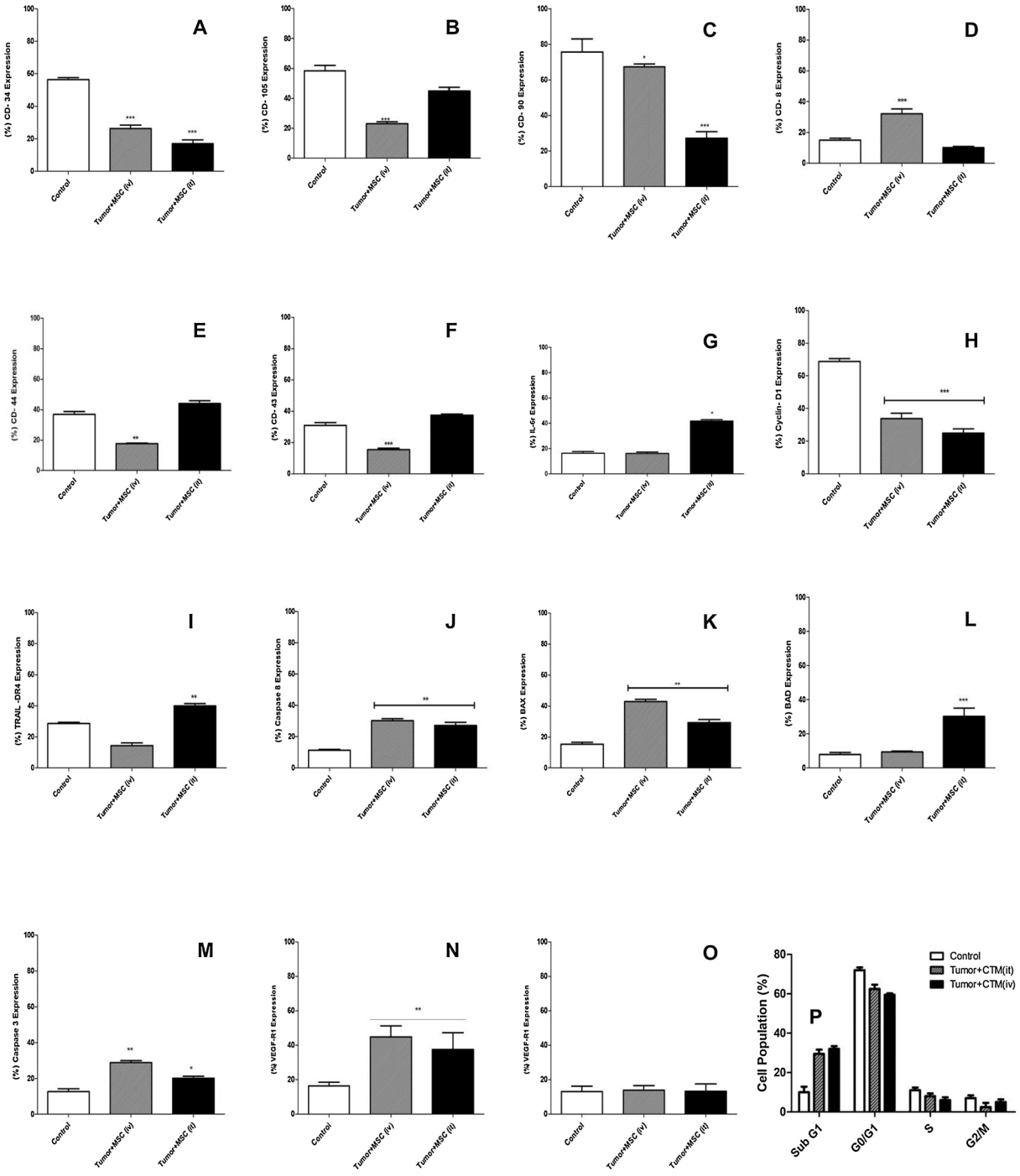

Fig. 3. Analysis of the expression levels of markers by flow cytometry. (A) CD34 expression. (B) CD105 expression. (C) CD90 expression. (D) CD8 expression. (E) CD44 expression. (F) CD43 expression. (G) IL-6 r protein expression. (H) Cyclin D1 protein expression. (I) TRAIL-DR4 receptor expression. (J) Caspase-8 protein expression. (K) Bax protein expression. (L) Bad protein expression. (M) Expression of the caspase-3 protein (N) VEGF-R1 expression. (O) VEGF-R2 expression. (P) Determination of cell cycle phase distribution. Values are expressed as mean ± SD standard deviation. Statistical significance level $p < 0.05$, ** $p < 0.01$ and *** $p < 0.001$.

the distribution profile of cell populations in the cell cycle phases: G0/G1, S phase, G2/M and fragmented DNA (Sub-G1). The number of cells in the sub-G1 phase increased significantly after the treatment period, relative to the control group. However, the percentage of cells in the G0/G1 phases therefore decreased significantly after the treatment period in the two treated groups. The percentage of cells in the synthesis and proliferative phase (S and G2/M), decreased significantly. The mean values for Synthesis phase were 11.5 ± 0.6% for the control group; 8.5 ± 0.7% for the Tumor + MSC (it) treated group and 6.5 ± 0.5% for the Tumor + MSC (iv) treated group. Only the Tumor + MSC (it) treated group showed a significant decrease in the G2/M phase, with a mean value of 2.9 ± 0.16% (Fig. 3P).

Histopathological changes in the organs of melanoma-bearing mice were evaluated at the end of treatment. It was observed that the animals in the control group had a dense conformation and a large number of neoplastic cells and the presence of atypical mitosis (Fig. 6A–B). The lymph node parenchyma presented alterations in its architecture, in which it was possible to observe the formation of a tumor mass and a large number of dispersed neoplastic cells (Fig. 4C–F). Tumor + MSC (it) treated group did not present obvious changes in spleen

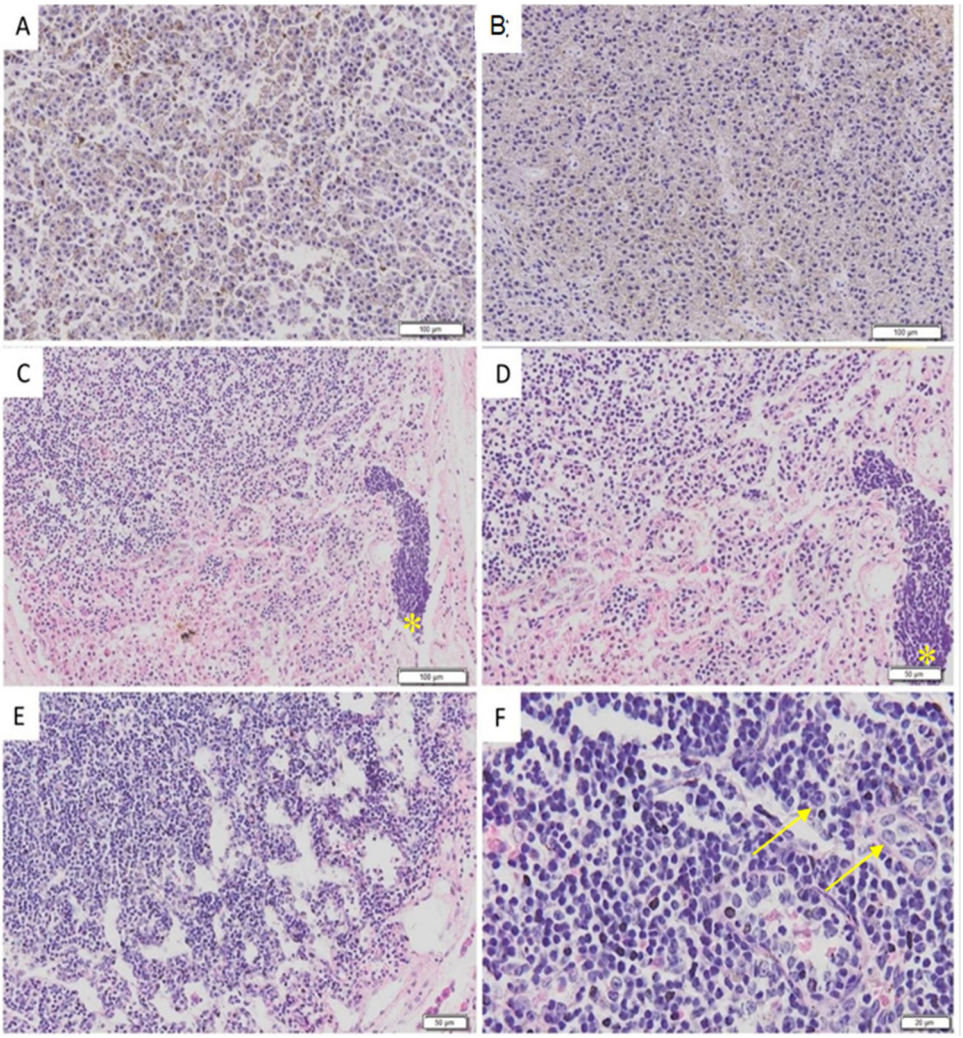

Fig. 4. Photomicrographs representative of the histological appearance of lymph nodes and tumor mass of C57BL / 6 J mice, with melanoma. (A, B) Architecture of the tumor mass. (C–F) Lymph node parenchyma. H & E staining. Tumor mass formation (asterisk); neoplastic cells (arrow).

architecture. There was also no tumor mass formation in the lymph nodes of these animals. Only a small number of atypically dispersed cells were visualized in the lymph node parenchyma (Fig. 5A–C). Microscopic analysis of the tumor mass of Tumor + MSC (it) treated group demonstrated that the treatment was able to induce the death of neoplastic cells, and it was possible to observe the presence of necrotic areas and apoptotic bodies in this tissue (Fig. 5D–F). In addition, it was possible to observe that Tumor + MSC (iv) treated group had evident changes in the lymph node parenchyma, even with formation of a tumor mass with foci of necrosis and apoptotic bodies (Fig. 6A–C). For both groups treated, Tumor + MSC (it) and Tumor + MSC (iv), we observed that the tumor mass of the animals' back showed large areas of necrosis and presence of apoptotic bodies, suggesting that the treatment is effective in inducing cell death in the tumor tissue (Fig. 6D–E).

4. Discussion

The genetics and biological behavior of murine melanoma are well known, as well as their histological characteristics, which are similar to human melanoma. When kept in culture, they show rapid growth. Moreover, transplantation in histocompatible animals can be carried out easily and through different inoculation routes. With high metastatic dissemination capacity, it can be easily seen in the skin and organs by the presence of melanin in high concentration, facilitating its observation in the varied interactions in the residual sites [19,20].

Our results, after treatment, showed a decrease in volume and tumor mass in animals treated with MSCs in both pathways, as confirmed by macroscopic and microscopic analysis of these animals after necropsy, when compared to the untreated control group.

In the anatomopathological analysis of the animals treated with MSCs, via (it) and (iv), a great variation of the coloration of the tumors was visualized, of colors ranging from black to shades of brown and white amelanotic, indicating populations of heterogeneous tumor cells, evidenced by the presence of nodular formation. A large neovascularization around these tumors can be seen under microscopy, being shown to be proportional to the size of the tumors.

Numerous studies have now focused on modified MSCs, where they supply antiangiogenic compounds to the target tissue, modulating the expression of chemokine genes (CXCL10, CXCL3, CXCL6 and CCL-2) without short-term side effects, but long-term administration. toxicity as well as poor blood supply [21–23]. But there are some limitations to the use of MSCs to reduce vascularization, as angiogenesis is a very complex process and inhibitors may result in hypoxia generating chemo and radi resistance, as intratumoral blood flow will be reduced [24].

Angiogenesis plays a role in progression and metastasis of melanoma. The vascular endothelial growth factor (VEGF) pathway plays a critical role in angiogenesis. VEGF signals primarily through receptor tyrosine kinases VEGF receptor 1 (VEGF-R1, flt-1) and 2 (VEGF- R2, flk2/kdr).VEGF signals through its receptor VEGFR1/flt-1 (R1) but is thought to mediate most of its angiogenic and proliferative effects through

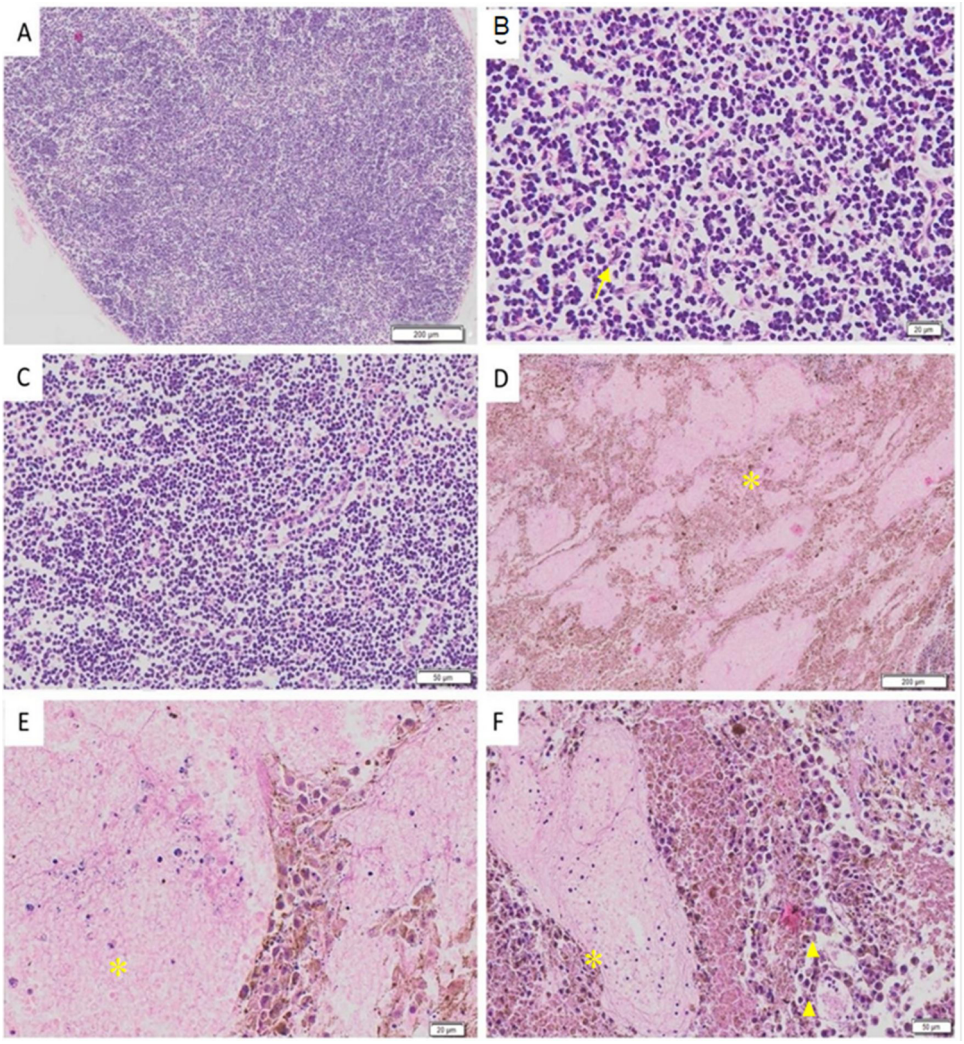

Fig. 5. Photomicrographs representative of the histological appearance of lymph nodes and tumor mass of C57BL / 6 J melanoma carriers treated with MSC at concentration 10^6, intratumorally, once a week for 28 days. (A–C) Lymph node parenchyma. (D–F). Tumor mass architecture. H & E staining. Neoplastic cells (arrow); areas with necrosis focus (asterisk); formation of apoptotic bodies (arrow head).

VEGFR2/flk-1/kdr (R2). In smaller melanoma studies, VEGFR2 and less commonly R1 expression was associated with disease aggression [25].

Migration of MSC cells to the tumor microenvironment improves inflammatory response, induction of stromal remodeling process and vasculogenesis. Migration is a process of multiple steps in vivo, and responsible for activation of MSCs. Sun el al, 2005 demonstrated the correlation between angiogenesis in melanoma. MSC have been found to transmigrate over the endothelial barrier and possess the ability to leave blood vessels after application. MSCs are able to migrate to both primary and metastatic tumor sites through associations with various chemokines and cytokines [26–28].

There was also a decrease in tumor cell infiltration in the parenchyma of the organs analyzed, as well as the formation of an area of extensive necrosis, with apoptotic bodies in the tumor mass, evidencing that the application of MSC may be promising for the treatment of metastatic melanoma.

A number of studies have demonstrated that once MSCs are incorporated into the tumor mass, they contribute with other cells such as myofibroblasts, endothelial cells, pericytes, and inflammatory cells to create a tumor microenvironment and influence in the change of morphology and proliferation rate [29,30].

It is worth mentioning that the inoculation pathways of the MSCs can influence both the response to the target, since they have different niches. After a tissue injury, certain inflammatory mediators are responsible for recruiting local stem cells [31,32]. For many experimental gastrointestinal tumors, the application by the endovenous pathway of modified MSCs has been shown to be more effective. Other studies have demonstrated that endovenous inoculation of MSCs isolated from adipose tissue was more efficient than the intraperitoneal route in the treatment of

induced colitis in C57BL/6 mice, leading to a reduction in clinical and histopathological severity. These results showed that MSCs can induce apoptosis in T cells resistant to colon inflammation [33]. Corroborating this fact, in this study, it was possible to verify that when treated by intratumor or intravenous, the behaviors and the responses were different regarding the expression of proteins involved in apoptosis, however, the pro-apoptotic effects of MSCs were more pronounced in the Tumor + MSC (iv).

The animals in the control group had anemic disorders, characterized by decreased erythrocytes and/or hemoglobin. It was expected that there would be reduction of erythrocytes in all the studied groups, mainly with the tumor growth in the animals. In both MSC treated groups, there was an increase in the number of reticulocytes in the circulating blood, thus, indicating a compensatory proliferative activity by the bone marrow, which could mean higher efficiency of the medullary response in the treated animals. These data corroborate with the results reported in the literature, and may be justified by the immunomodulatory capacity that MSCs play in tumor tissues [34,35]. On the other hand, the total number of leukocytes increased significantly in

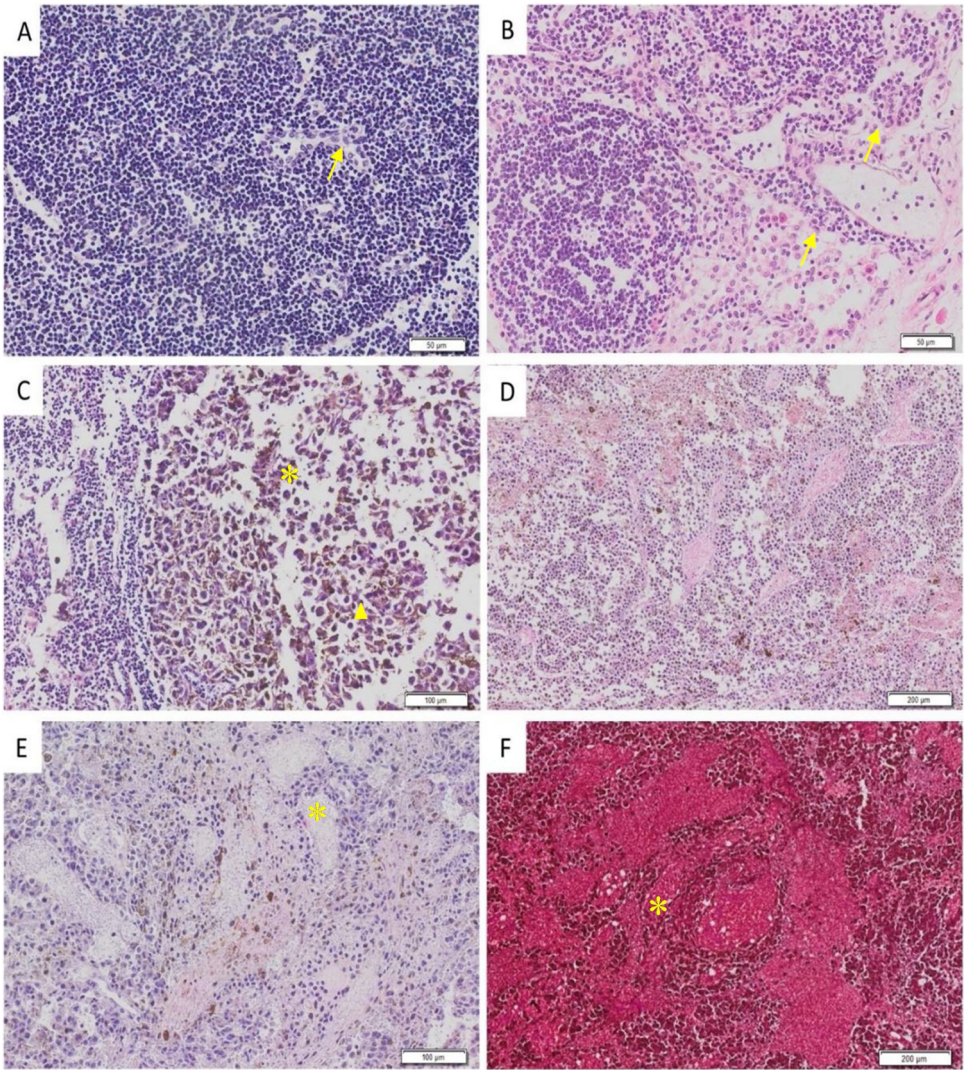

Fig. 6. Photomicrographs representative of the histological appearance of the lymph nodes and tumor mass of C57BL / 6 J melanoma carriers treated with MSC at concentration 10^6 by the intravenous route once a week for 28 days. (A–C) Lymph node parenchyma. (D–F) Architecture of the tumor mass. H & E and Masson's Trichrome staining (F). Neoplastic cells (arrow); areas with necrosis focus (asterisk); formation of apoptotic bodies (arrow head).

both treated groups, whereas the control group had leukopenia. The increase in the total number of leukocytes may be related to the decrease in tumor mass after the treatment period with MSC. In the leukocyte differential count, it was possible to observe that the number of lymphocytes decreased after the treatment period. Initial studies report that patients with normal lymphocyte counts have a better prognosis than patients with reduced lymphocyte counts [36]. The administration of MSCs modified the monocyte differentiation on tumor microenvironments by modulating the cell cycle, suggesting that MSC-induced immunosuppression might be the consequence of a more general anti-proliferative effect.

Post-treatment analyzes, by flow cytometry, showed that MSC treatment provided significant changes in the expression of proteins related to the control and progression of cell proliferation.

Ahn et al. (2015) have observed similar effects of adipose tissue derived MSC in conditioned media on human melanoma lineage A375SM and A375 P. Tumors were inoculated into Balb/c and nude mice and tumor size was measured. In the study in question, MSCs, derived from adipose tissue, altered cell distribution in cell cycle phases and induced apoptosis of tumor cells in vitro by the fact that MSCs migrated efficiently to the tumor mass and virtually suppressed their growth.

Recent studies have reported that clinical administration of MSCs has shown no serious adverse effects in various animal experiments. But the issue of safe long-term use of MSCs is still a critical point that needs to be addressed before its use in clinical therapy in humans, other factors such as the potential risk of intrinsic mechanisms that may induce tumorigenesis, metastasis and drug resistance., in addition to a profibrogenic potential as seen in human BM-MSCs-induced liver fibrosis has recently been seen in a study [37–40].

Thus, in this study, it was possible to show that the treatment with MSCs led to the control of cell proliferation in B16F10 murine melanoma.

Funding

DAM Supported financial CNPq (Process number 306124/2015-7)

Declaration of Competing Interest

The authors declare that there are no conflicts of interest.

Acknowledgement

Not applicable.

Appendix A

See Figs. A1, A2, A3.

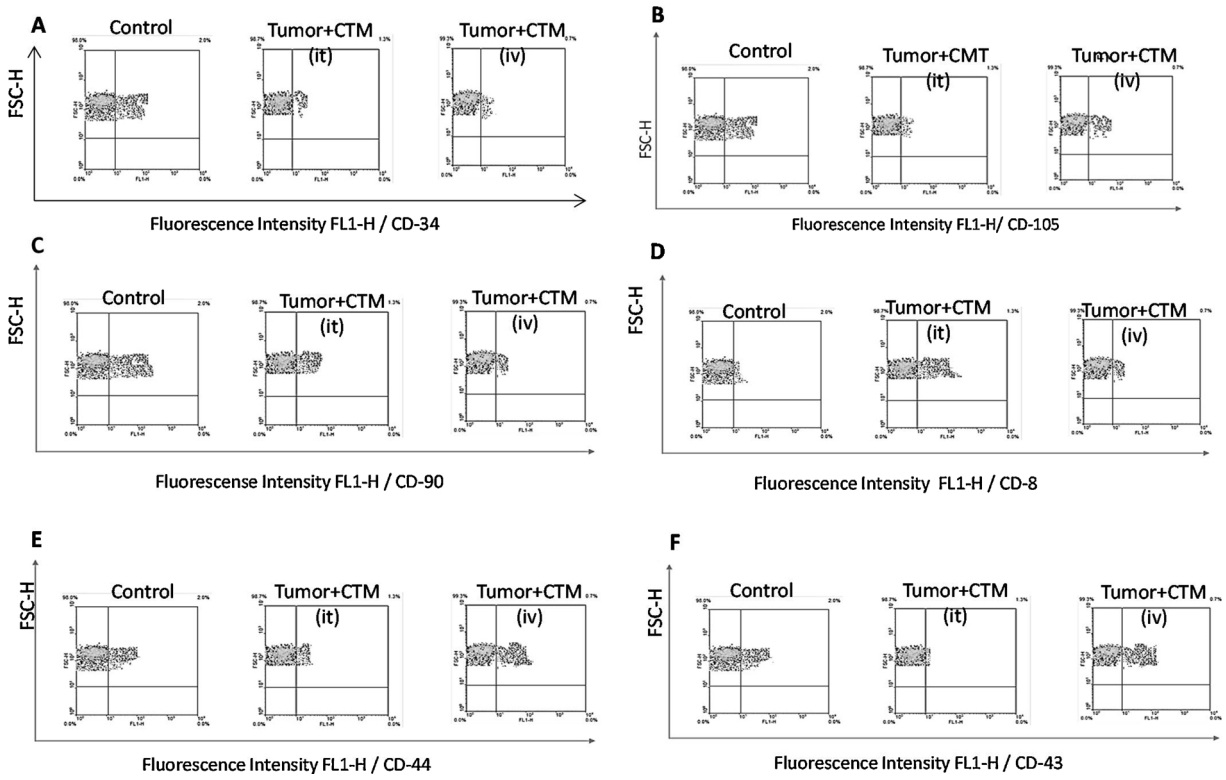

Fig. A1. Representative dot plots show the cell number distribution in relation to fluorescence intensity of markers by flow cytometry. (A) CD34, (B) CD105, (C) CD90, (D) CD8, (E) CD44, (F) CD43.

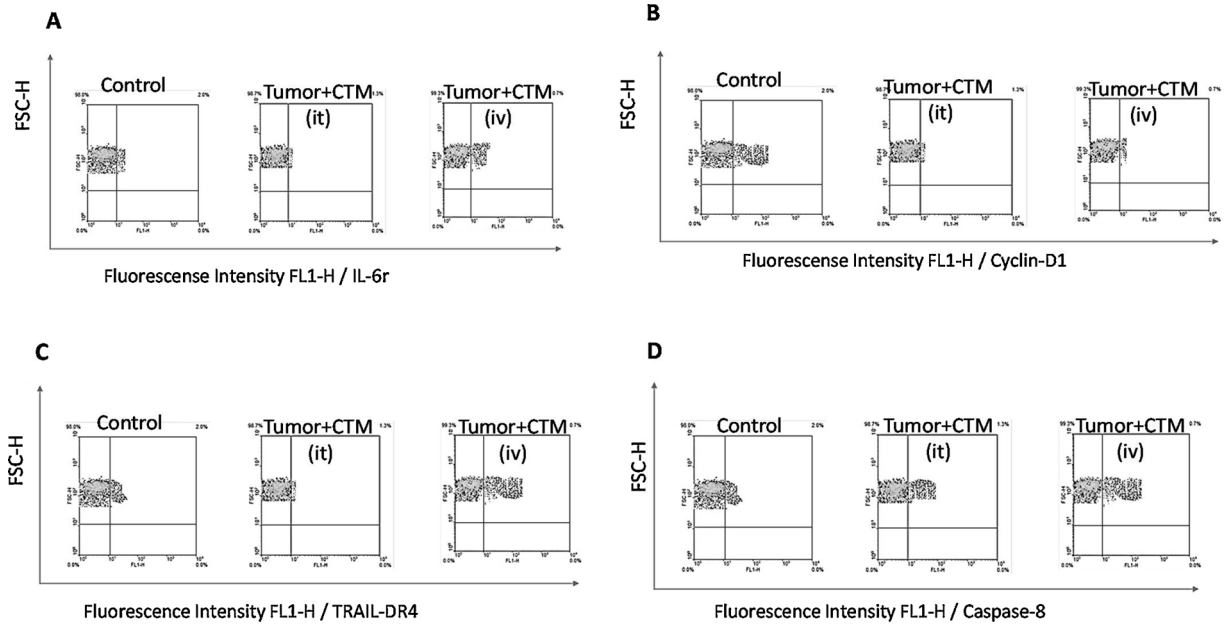

Fig. A2. Representative dot plots show the cell number distribution in relation to fluorescence intensity of markers by flow cytometry. (A) IL-6 r, (B) Cyclin D1, (C) TRAIL-DR4, (D) Caspase-8.

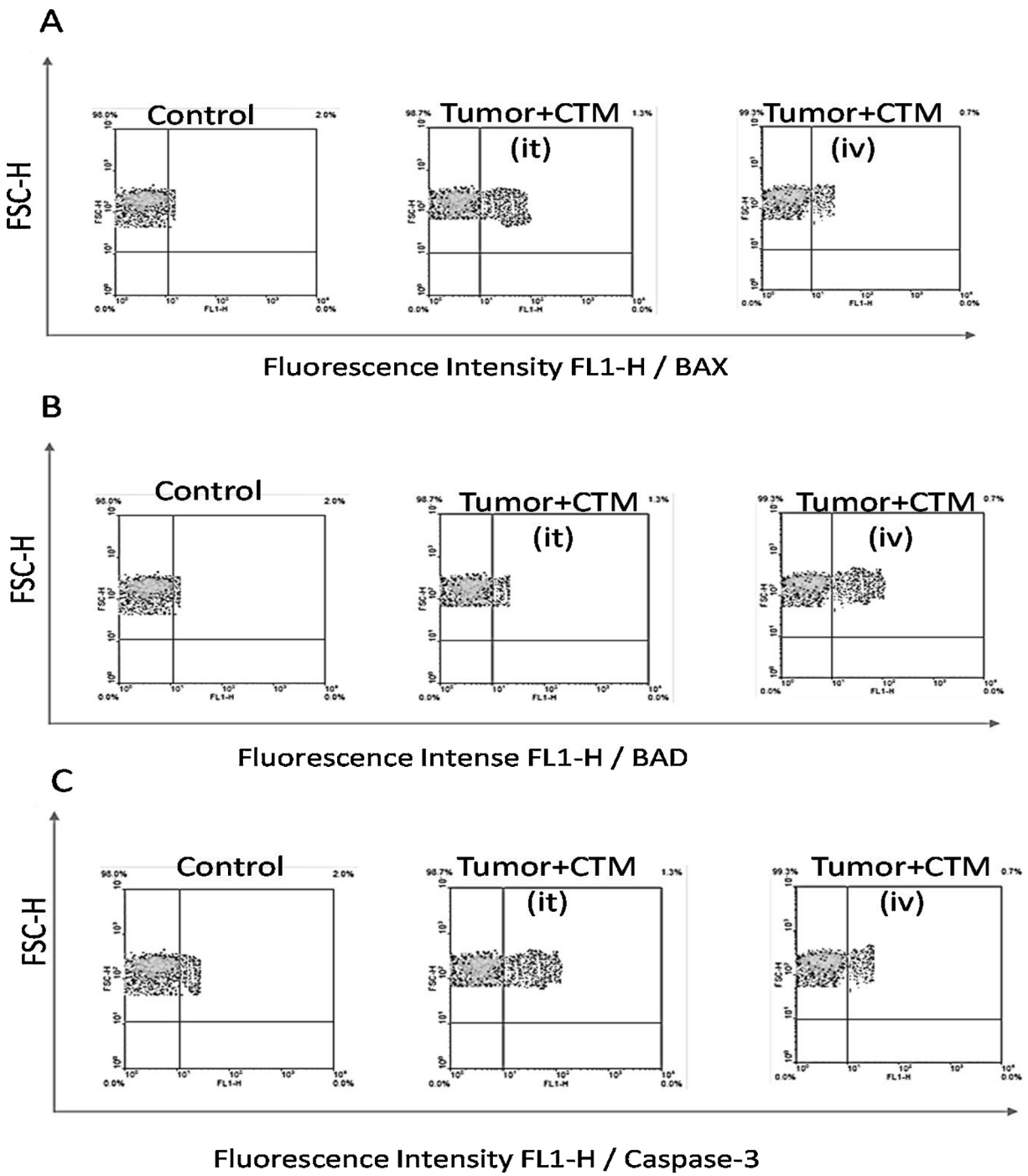

Fig. A3. Representative dot plots show the cell number distribution in relation to fluorescence intensity of markers by flow cytometry. (A) BAD, (B) BAX, (C) Caspase-3.

References

[1] T. Schatton, M.H. Frank, Cancer stem cells and human malignant melanoma, Pigment Cell Melanoma Res. 21 (1) (2008) 39–55.

[2] J.L. Bolognia, J.V. Schaffer, L. Cerroni (Eds.), Dermatology E-Book, 4ª ed, Elsevier Health Sciences, New York, 2017.

[3] J. Read, Recent advances in cutaneous melanoma: towards a molecular model and targeted treatment, Australas. J. Dermatol. 54 (3) (2013) 163–172.

[4] A.G. Richetta, V. Silvestri, S. Giancristoforo, P. Rizzolo, S. D'Epiro, V. Graziano, et al., Mutational profiling in melanocytic tumors: multiple somatic mutations and clinical implications, Oncology 86 (2) (2014) 104–108.

[5] Instituto Nacional do Câncer – INCA, Tipos de câncer: pele não melanoma, (2018) http://www2.inca.gov.br/wps/wcm/connect/tiposdecancer/site/home/pele_nao_melanoma.

[6] R.L. Siegel, K.D. Miller, A. Jemal, Cancer statistics, 2018, CA Cancer J. Clin. 67 (1) (2017) 7–30.

[7] A.M. Sortino-Rachou, M.P. Curado, M. de C Cancela, Melanoma cutâneo na América Latina: estudo descritivo de base populacional, Cad Saúde Pública 27 (3) (2011) 565–572.

[8] Instituto Oncoguia, Câncer de pele basocelular e espinocelular, (2016) http://www.oncoguia.org.br/cancer-home/cancer-de-pele-basocelular-e-espinocelular/30/146.

[9] A. Corcione, F. Benvenuto, E. Ferretti, D. Giunti, V. Cappiello, F. Cazzanti, et al., Human mesenchymal stem cells modulate B-cell functions, Blood 107 (1) (2006) 367–372.

[10] A.J. Nauta, W.E. Fibbe, Immunomodulatory properties of mesenchymal stroma cells, Blood 110 (10) (2007) 3499–3506.

[11] E. Fuchs, T. Tumbar, G. Guasch, Socializing with the Neighbors: stem cells and their

niche, Cell 116 (6) (2004) 769–778.
[12] M.F. Corsten, K. Shah, Therapeutic stem-cells for cancer treatment: hopes and hurdles in tactical warfare, Lancet Oncol. 9 (2008) 376–384, https://doi.org/10.1016/S1470-2045(08)70099-8.
[13] A.K. Teo, L. Vallier, Emerging use of stem cells in regenerative medicine, Biochem. J. 428 (2010) 11–23, https://doi.org/10.1042/BJ20100102.
[14] Ranjeet Singh Mahla, Stem cells applications in regenerations medicine and disease therapeutics, Int. J. Cell Biol. 6940283 (2016), https://doi.org/10.1155/2016/6940283 24 P..
[15] Sergio P. Bydlowski, Adriana A. Bebes, Luciana M.F. Maselli, Felipe L. Janz, Biological characteristics of mesenchymal stem cells, Rev. Bras. Hematol. Hemoter. 31 (suppl.1) (2009) 25–35, https://doi.org/10.1590/S1516-84842009005000038 Epub June 05, 2009. ISSN 1516-8484.
[16] Samira Yarak, Oswaldo Keith Okamoto, Human adipose-derived stem cells: current challenges and clinical perspectives, An. Bras. Dermatol. [online] 85 (5) (2010) 647–656, https://doi.org/10.1590/S0365-05962010000500008 ISSN 0365-0596.
[17] M.A. Zago, D.T. Covas, Pesquisas com células-tronco: aspectos científicos, éticos e sociais, Seminário do Instituto Fernando Henrique Cardoso, São Paulo, Instituto Fernando Henrique Cardoso, Anais São Paulo, 2004, p. 23p.
[18] W.J. Ennis, A. Sui, A. Bartholomew, Stem cells and healing: impact on inflammation, Adv. Wound Care (New Rochelle) 2 (7) (2013) 369–378.
[19] C.W. Beattie, R. Tissot, M. Amoss, Experimental models in human melanoma research: a logical perspective, Sem Oncol 15 (6) (1988) 500–511.
[20] Cherly Lee D. ebertinga, David P. Shrayera, Janet Butmarca, Vicent Falangaa, Histologic progresseion of B16 F10 metastatic melanoma in C57BL/6 mice over a six week time period: distant metastases before local growth, J. Dermatol. 31 (2004) 299–304.
[21] M. Ghaedi, M. Soleimani, N.M. Taghvaie, M. Sheikhfatollahi, K. Azadmanesh, A.S. Lotfi, et al., Células-tronco mesenquimais como veículos para entrega direcionada de proteína antiangiogênica a tumores sólidos, J. Gene Med. 13 (2011) 171–180, https://doi.org/10.1002/jgm.1552.
[22] M.M. Najafabadi, K. Shamsasenjan, P. Akbarzadehlaleh, The angiogenic chemokines expression profile of myeloid cell lines Co-cultured with bone marrow-derived mesenchymal stem cells, Cell J. 20 (19) (2018), https://doi.org/10.22074/cellj.2018.4924.
[23] M. Toi, S. Hoshina, T. Takayanagi, T. Tominaga, Association of vascular endothelial growth factor expression with tumor angiogenesis and with early relapse in primary breast cancer, Cancer Sci. 85 (1994) 1045–1049, https://doi.org/10.1111/j.1349-7006.1994.tb02904.x.
[24] M.R. Javan, A. Khosrojerdi, S.M. Moazzeni, New insights into implementation of mesenchymal stem cells in cancer therapy: prospects for anti-angiogenesis treatment, Front. Oncol. (2019) 9, https://doi.org/10.3389/fonc.2019.00840.
[25] Q. Bao, Y. Zhao, H. Niess, C. Conrad, B. Schwarz, K.W. Jauch, et al., Mesenchymal stem cell- based tumor-targeted gene therapy in gastrointestinal cancer, Stem Cells Dev. 21 (13) (2012) 2355–2363.
[26] N. Ferrara, H.P. Gerber, J. Le Couter, The biology of VEGF and its receptors, Nat. Med. 9 (2003) 669–676.
[27] B. Sun, S. Zhang, C. Ni, D. Zhang, Y. Liu, W. Zhang, X. Zhao, C. Zhao, M. Shi, Correlation between melanoma angiogenesis and the mesenchymal stem cells and endothelial progenitor cells derived from bone marrow, Stem Cells Dev. (14) (2005) 292–298.
[28] A. Schmidt, D. Ladage, C. Steingen, K. Brixius, T. Schinkothe, F.J. Klinz, R.H. Schwinger, U. Mehlhorn, W. Bloch, Mesenchymal stem cells transmigrate over the endothelial barrier, Eur. J. Cell Biol. (85) (2006) 1179–1188.
[29] H. Mirzaei, A. Sahebkar, A. Avan, M.R. Jaafari, R. Salehi, H. Salehi, H. Baharvand, A. Rezaei, J. Hadjati, J.M. Pawelek, et al., Application of mesenchymal stem cells in melanoma: a potential therapeutic strategy for delivery of targeted agents, Curr. Med. Chem. (23) (2016) 455–463.
[30] F.T. Martin, R.M. Dwyer, J. Kelly, S. Khan, J.M. Murphy, C. Curran, N. Miller, E. Hennessy, P. Dockery, F.P. Barry, T. O'Brien, M.J. Kerin, Potential role of mesenchymal stem cells (MSCs) in the breast tumour microenvironment: stimulation of epithelial to mesenchymal transition (EMT), Breast Cancer Res. Treat. (2) (2010) 317–326.
[31] B.D. Roorda, A. ter Elst, W.A. Kamps, E.S. de Bont, Bone marrow-derived cells and tumor growth: contribution of bone marrow-derived cells to tumor microenvironments with special focus on mesenchymal stem cells, Crit. Rev. Oncol. Hematol. (3) (2009) 187–198.
[32] F.C. Gonçalves, N. Schneider, F.O. Pinto, F.S. Meyer, F. Visioli, B. Pfaffenseller, et al., Intravenous vs intraperitoneal mesenchymal stem cells administration: what is the best route for treating experimental colitis? World J. Gastroenterol. 20 (48) (2014) 18228–18239.
[33] S. Ramdasi, S. Sarang, C. Viswanathan, Potential of mesenchymal stem cell based application in cancer, Int. J. Hematol. Stem Cell Res. 9 (2) (2015) 95–103.
[34] R. Abdi, P. Fiorina, C.N. Adra, M. Atkinson, M.H. Sayegh, Immunomodulation by mesenchymal stem cells: a potential therapeutic strategy for type 1 diabetes, Diabetes 57 (7) (2008) 1759–1767.
[35] M.G. Bernengo, F. Lisa, M. Meregalli, A. De Matteis, G. Zina, "The prognostic value of T- lymphocyte levels in malignant melanoma". A five-year follow-up, Cancer 52 (10) (1983) 1841–1848.
[36] J.O. Ahn, Y.R. Coh, H.W. Lee, I.S. Shin, S.K. Kang, H.Y. Youn, Human adipose tissue-derived mesenchymal stem cells inhibit melanoma growth in vitro and in vivo, Anticancer Res. 35 (1) (2015) 159–168.
[37] M. Jaafari, R. Salehi, H. Salehi, et al., Application of mesenchymal stem cells in melanoma: a potential therapeutic strategy for delivery of targeted agents, Curr. Med. Chem. 23 (5) (2016) 455–463.
[38] C. Uder, S. Brückner, S. Winkler, H.M. Tautenhahn, B. Christ, Mammalian MSC from selected species: features and applications, Cytometry 93 (2018) 32e49.
[39] L. Barkholt, E. Flory, V. Jekerle, S. Lucas-Samuel, P. Ahnert, L. Bisset, et al., Risk of tumorigenicity in mesenchymal stromal cell-based therapies–bridging scientific observations and regulatory viewpoints, Cytotherapy 15 (2013) 753e9.
[40] F.P. Russo, M.R. Alison, B.W. Bigger, E. Amofah, A. Florou, F. Amin, et al., The bone marrow functionally contributes to liver fibrosis, Gastroenterology 130 (2006) 1807e21.